Chinese Chemical Letters 33 (2022) 1604–1608

Contents lists available at ScienceDirect

Chinese Chemical Letters

journal homepage: www.elsevier.com/locate/cclet

Chemical chaperone delivered nanoscale metal–organic frameworks as inhibitor of endoplasmic reticulum for enhanced sensitization of thermo-chemo therapy

Xiaoyan Ma[a,b], Qiong Wu[a,c], Longfei Tan[a,c,*], Changhui Fu[a,c], Xiangling Ren[a,c], Qijun Du[a,c], Lufeng Chen[d], Xianwei Meng[a,c,*]

[a] *Laboratory of Controllable Preparation and Application of Nanomaterials, Technical Institute of Physics and Chemistry, Chinese Academy of Sciences, Beijing 100190, China*
[b] *Graduate School of Bio-Applications and Systems Engineering, Tokyo University of Agriculture and Technology, Kokyo 184-8588, Japan*
[c] *CAS Key Laboratory of Cryogenics, Technical Institute of Physics and Chemistry, Beijing 100190, China*
[d] *First Clinical Medical School and First Hospital, Shanxi Medical University, Taiyuan 030001, China*

ARTICLE INFO

Article history:
Received 14 June 2021
Revised 23 September 2021
Accepted 23 September 2021
Available online 30 September 2021

Keywords:
Metal–organic frameworks
Biodegradable
Chemotherapy
Thermotherapy
Microwave

ABSTRACT

Thermotherapy and chemotherapy have received extensive attention to tumor treatment. However, thermal tolerance and drug resistance severely limit clinical effect of tumor therapy owing to endoplasmic reticulum (ER) stress. Reducing thermal tolerance and drug resistance of tumors is an urgent challenge to be solved. In this work, we design a nanoplatform of PBA-Dtxl@MIL-101 as an ER inhibitor. Amino functionalized Fe-metal organic framework (MIL-101) nanoparticles are synthesized as pH and microwave (MW) dual stimuli-responsive drug delivery system. Then, the chemical chaperones of 4-phenylbutyric acid (PBA) and antineoplastic drug Docetaxel (Dtxl) were successfully loaded into MIL-101 nanoparticles to form PBA-Dtxl@MIL-101 nanoparticles. Furthermore, PBA-Dtxl@MIL-101 nanoparticles exhibit inhibitor effect of ER stress through upregulating caspase 9 proteins and reduce thermal tolerance by downregulating HSP 90. It was demonstrated that the therapy sensitized by PBA-Dtxl@MIL-101 nanoparticles obviously destroyed tumor cells, showing simultaneously enhanced thermo-chemo therapy.

Thermotherapy and chemotherapy have been extensively investigated as curative therapeutic methods for tumors. Thermotherapy presents several attractive advantages, especially noninvasive manner and considerably lower side effects, approving for tumor treatment compared with conventional treatments [1]. However, thermotherapy may cause thermal tolerance of tumor cells due to stress-inducible proteins, such as heat shock proteins (HSP), which is a bottleneck for successful thermotherapy and may even lead to tumor recurrence [2]. Chemotherapy, as a conventional therapeutic method for effectively destroying tumor cells, has always been some crucial problems of poor targeting, quick deactivations and defecations. Importantly, drug resistance often occurs due to unfolded proteins and the overexpression of ATP-dependent drug efflux pumps [3,4]. However, no breakthrough can be drove for more superior anti-tumor efficacy due to the drug resistance and thermal tolerance.

It is well known that endoplasmic reticulum (ER) is a crucial site to produce proteins for benefiting cell survival. When subjecting to exogenous stimulation, misfolded or unfolded proteins are accumulated in the ER, which causes ER stress signaling for further preventing cancer cells from necrosis in the hostile environment [5]. Therefore, eliminating ER stress is a pivotal strategy to reverse thermal tolerance and drug resistance. In order to eliminate ER stress, chemical chaperones as one of chaperones, play a significant role. Because chemical chaperones can give assistance for folding proteins and preventing unfolded and incomplete proteins from aggregating, and assisting in defective proteins to fold in the ER lumen [6]. Hence it can reduce thermal tolerance to tumor cells *via* inhibiting HSP processing [7,8]. Additionally, affinity binding with unfolded or misfolded proteins in ER can enhance the sensitization of drugs to tumor cells in chemotherapy [9]. Proper integration of resistance reversal agents may thus be critical to improve antitumor efficacy of whether thermotherapy or chemotherapy. However, the non-selectivity and potential toxicity of free drugs further

* Corresponding authors at: Laboratory of Controllable Preparation and Application of Nanomaterials, Technical Institute of Physics and Chemistry, Chinese Academy of Sciences, Beijing 100190, China.
E-mail addresses: longfeitan@mail.ipc.ac.cn (L. Tan), mengxw@mail.ipc.ac.cn (X. Meng).

https://doi.org/10.1016/j.cclet.2021.09.084
1001-8417/

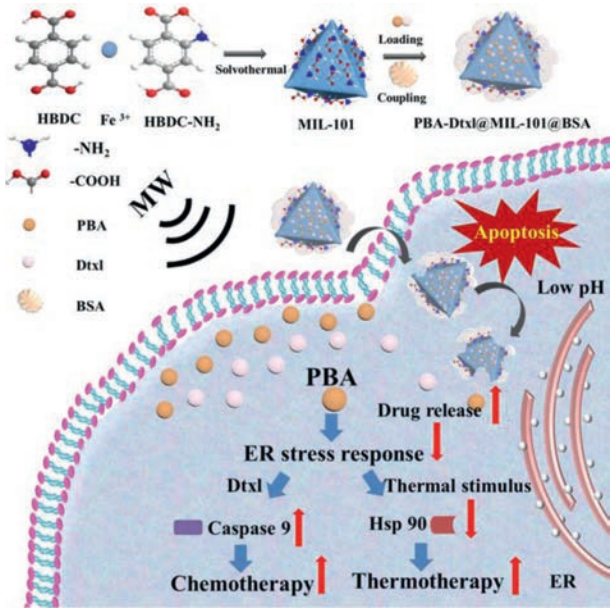

Scheme 1. Schematic illustration of PBA-Dtxl@MIL-101@BSA nanoparticles synthesis and combination therapy of thermotherapy and chermotherapy.

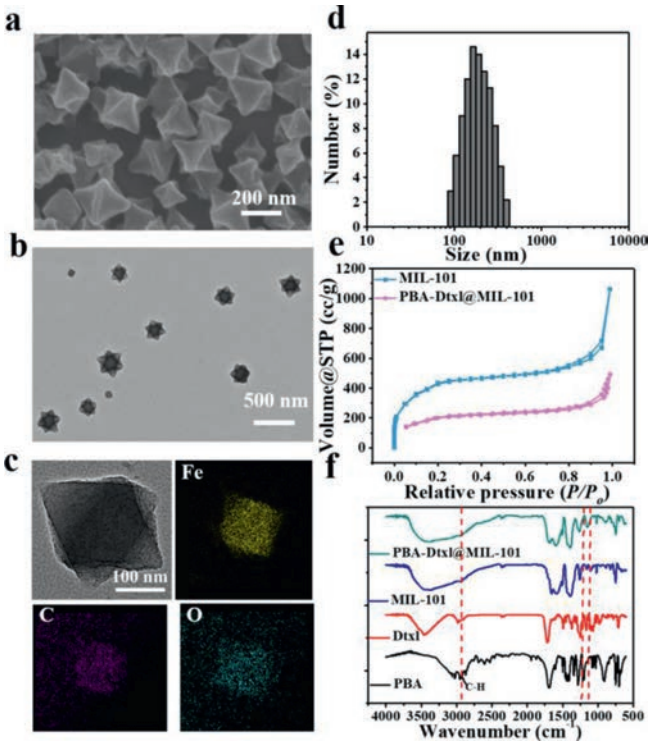

Fig. 1. The characterization of PBA-Dtxl@MIL-101@BSA nanoparticles. SEM (a) and TEM (b) images of MIL-101 nanoparticles. (c) HRTEM-mapping images of MIL-101 nanoparticles and the elemental mapping of Fe, C, O. (d) The average hydrodynamic diameter of MIL-101 nanoparticles. (e) N_2 isothermal adsorption–desorption curves of PBA-Dtxl@MIL-101 nanoparticles and MIL-101 nanoparticles. (f) FT-IR spectrum of PBA, Dtxl, MIL-101, PBA-Dtxl@MIL-101 nanoparticles.

limit the clinical application. Consequently, it is highly desired for design an effective agent with enhanced tumor-specific accumulation, prolonged blood circulation and reduced toxicity.

Recently, metal organic framework (MOF) materials for tumor therapy have attracted widespread attention due to the advantages of good biocompatibility, high loading capacity and biodegradability over traditional drug delivery nanocarriers [10,11]. It is worth mentioning, taking the remarkable responsiveness on pH value [12], light [13], ultrasound [14], redox and magnetic field [15], MOF-based smart nanocarriers have been developed [16]. Microwave (MW) is considered as an ideal external stimulation with advantages of low side effect and deep penetration [17,18]. Designing MW sensitizing nanoagents has great potential to realize noninvasive and controllable manner.

Inspired by the aforementioned aims, we have designed a pH and MW dual stimuli-responsive nanoplatform that further acted as an ER inhibitor for enhancing chemotherapy and thermotherapy. Docetaxel (Dtxl) is chosen as a traditional antineoplastic drug. 4-Phenylbutyric acid (PBA) as chemical chaperone is used to alleviate ER proteotoxicity and avoids unfolded protein response. Amino functionalized Fe-metal organic framework (MIL-101) nanoparticles were synthesized to obtain PBA-Dtxl@MIL-101 nanoparticles with both pH and MW stimuli-response. PBA-Dtxl@MIL-101 nanoparticles showed obvious inhibition of ER stress by downregulating HSP 90 and further enhanced sensation to tumor cells by upregulating caspase 9 (Scheme 1). In contrast to conventional thermotherapy and chemotherapy, this smart drug delivery system as ER stress inhibitor significantly obstructs tumor cells survival for maximizing treatment efficacy and minimizing treatment resistance.

The solvothermal method was adopted to synthesize MIL-101 nanoparticles [19]. The morphology of MIL-101 nanoparticles was showed from scanning electron microscopy (SEM) image (Fig. 1a) and transmission electron microscopy (TEM) image (Fig. 1b). The dynamic light scattering (DLS) was used to test the average hydrodynamic diameter of MIL-101 nanoparticles, exhibiting 160.9 nm (Fig. 1d). The homogeneous distributions of Fe, C, O in MIL-101 nanoparticles were exhibited by the EDS-elemental mapping (Fig. 1c) and the feature elements in MIL-101 nanoparticles were showed by EDS (Fig. S1 in Supporting information). The specific surface area of MIL-101 nanoparticles was 1586.523 m^2/g (Fig. 1e) and the average micropore diameter was 1.658 nm (Fig. S2a in Supporting information), which was suitable for drug carriers. Moreover, the zeta potential value of MIL-101 nanoparticles was 7.18 mV. Dtxl possessing hydrophobicity and zeta potential value of –13.7 mV, has absorbability with MIL-101 nanoparticles *via* electrostatic interaction, which promoted Dtxl to load into MIL-101 nanoparticles. PBA possessed high solubility in ethanol at room temperature. Thus, PBA and Dtxl dispersed in ethanol were loaded into MIL-101 nanoparticles to obtain PBA-Dtxl@MIL-101 nanoparticles. The specific surface area of PBA-Dtxl@MIL-101 nanoparticles was 717.8 m^2/g and average micropore diameter was 1.409 nm, which less than surface area and average micropore diameter of MIL-101 nanoparticles, indicating that PBA and Dtxl were loaded successfully (Fig. S2b in Supporting information). As-made PBA-Dtxl@MIL-101 nanoparticles were further evaluated by the fourier transform infrared spectra. Fig. 1f showed the main characteristic peaks of PBA and Dtxl. The characteristic peak of PBA was 2927 cm^{-1}, exhibiting C–H stretching bands [20]. The characteristic peak of Dtxl was from 1275 cm^{-1} to 1060 cm^{-1}, showing many tertiary alcohol structures in Dtxl. It indicated that PBA and Dtxl were loaded into MIL-101 nanoparticles to successfully obtain PBA-Dtxl@MIL-101 nanoparticles. To improve the high biocompatibility of PBA-Dtxl@MIL-101 nanoparticles, bovine serum albumin (BSA) was coupled with the surface of PBA-Dtxl@MIL-101 nanoparticles. SEM and TEM images of PBA-Dtxl@MIL-101@BSA showed that BSA was wrapped on surface of PBA-Dtxl@MIL-101@BSA, exhibiting BSA shell on the surface of PBA-Dtxl@MIL-101 nanoparticles (Fig. S3 in Supporting information). Stability of PBA-Dtxl@MIL-101@BSA were evaluated in Supporting information (Fig. S4 in Supporting information). Above all, PBA-Dtxl@MIL-101@BSA nanoparticles were synthesized successfully, which would be suitable for subsequent experiments.

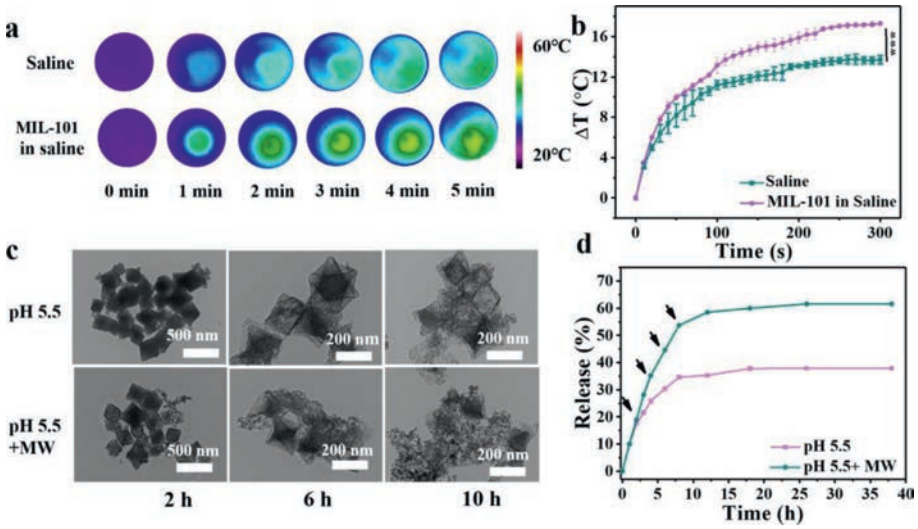

Fig. 2. The evaluation of MW fever-type heating response of MIL-101 nanoparticle and double stimuli-responsive drug delivery system promoting drug releasing experiment *in vitro*. (a) Heat curves of MIL-101 nanoparticles in saline and saline with MW stimulus. (b) Temperature change process of saline and MIL-101 nanoparticles dispersing in saline by FLIR images. (c) TEM degradable images of Dtxl@MIL-101 nanoparticles in pH 5.5 PBS, pH 5.5 PBS with MW stimulus at different time points (2, 6, 10 h). (d) The drug release curve of Dtxl@MIL-101 nanoparticles ($^{***}P < 0.001$)

During the MW heat response experiment, when dispersing MIL-101 nanoparticles in saline, MIL-101 nanoparticles with high specific surface area result in the rise of temperature due to ion collision. In order to reach the ideal temperature, 5 mg/mL of MIL-101 nanoparticles dispersed in saline and the saline as control group were treated with MW stimulus at 0.6 W for 5 min. As shown in Fig. 2b, the temperature change of saline, MIL-101 nanoparticles were 13.7 °C, 17.3 °C, indicating MIL-101 nanoparticles realized MW heating response. The temperature change process was recorded by forward-looking infrared (FLIR) imaging, Fig. 2a showed the temperature change process of saline, MIL-101 nanoparticles with MW stimulus. The result confirmed that MIL-101 nanoparticles possessed MW response. Thus MIL-101 nanoparticles were employed for fever-type heating [21].

MIL-101 nanoparticles could load more Dtxl due to electrostatic interaction, thus MIL-101 nanoparticles were idea choice as drug carriers due to MIL-101 nanoparticles possessed porous structure and excellent dispersity in ethanol. The drug loading capacity of Dtxl in MIL-101 nanoparticles reached up to 33.2% according to drug-loaded curve of UV-vis absorption of Dtxl at 229 nm (Fig. S5a in Supporting information). However, Dtxl loaded into MIL-101 nanoparticles was limited to release due to its hydrophobicity. Therefore, it was crucial to increase the releasing drug efficiency. It was favorable for Dtxl to release due to MIL-101 nanoparticles degrading in acidic buffer [22]. Moreover, the release efficiency of Dtxl was obviously increased under MW stimulus (0.6 W for 5 min). It achieved dual stimuli-responsive drug delivery system. When incubating Dtxl@MIL-101 nanoparticles in acid phosphate buffer (pH 5.5 PBS) for 10 h, the structure of Dtxl@MIL-101 nanoparticles exhibited slow degradation tendency. Dtxl@MIL-101 nanoparticles were incubating in acid phosphate buffer (pH 5.5 PBS) for 10 h with MW stimulus (0.6 W for 5 min) at 2, 6 and 10 h points, Dtxl@MIL-101 nanoparticles degraded quickly. Under MW stimulus, the structure of Dtxl@MIL-101 was collapsed rapidly, indicating the release rate of Dtxl would increase significantly (Fig. 2c). As Fig. S5b (Supporting information) shown that the standard curve of drug release was $A = 0.00594C + 0.10221$, and the correlation coefficient was 0.9999. Based on MIL-101 nanoparticles responsing for pH and MW stimulus, the release of Dtxl was explored under different conditions (pH 5.5 PBS, pH 5.5 PBS with MW stimulus) (Fig. 2d). Drug release time from 1, 2, 3, 4 to 38 h, UV-vis absorption was used to determine the concentration of Dtxl. The result confirmed that the release rate of Dtxl was 37.9% in pH 5.5 PBS after incubating for 38 h. While the release rate of Dtxl was up to 61.6% with MW stimulus at different time points (2, 4, 6, 8 h), indicating the release rate of Dtxl was increased by 23.7%. The result confirmed that double stimuli-responsive drug delivery system could promote Dtxl to release, which was potential for tumor treatment.

As shown in Fig. S10a (Supporting information), the drug release was further verified in 4T1 cells. The 4T1 cells were incubated with different concentrations of MIL-101@BSA and Dtxl@MIL-101@BSA nanoparticles (3.125, 6.25, 12.5, 25, 50, 100, 200 μg/mL) for 24 h, then the cell viability was evaluated by MTT assay. The cell viability of 4T1 cells treated with Dtxl@MIL-101@BSA was lower than cells treated by MIL-101@BSA at the same concentration. Especially, the cell viability of 4T1 cells treated with 200 μg/mL of Dtxl@MIL-101@BSA was 67.2%, indicating that Dtxl@MIL-101@BSA could effectively release Dtxl to destroy tumor cells. Thus Dtxl@MIL-101@BSA nanoparticles could further employ for tumor therapy *in vivo*.

It is well known that chaperones could prevent unfolded and incomplete proteins from aggregating and assisting in defective proteins to fold in the ER lumen. Chemical chaperones were constituted by small molecular weight compounds, which could give assistance for folding resistance and stability of proteins [23,24]. Therefore, chaperones could eliminate cell resistance for enhancing sensitization of cells in chemotherapy. In this work, PBA approved by Food and Drug Administration were chosen as chemical chaperones, preventing misfolded proteins from aggregating in the ER lumen to alleviate ER proteotoxicity and avoiding unfolded protein response [25]. PBA and Dtxl loading capacity of MIL-101 reached up to 31.3% and 33.2% according to the UV-vis absorption of PBA and Dtxl at 268 nm and 229 nm (Fig. S9 in Supporting information). It has reported that PBA as ER stress inhibitor could significantly enhanced the cell apoptosis of the drugs cisplatin-treated cells. Thence, it enhanced sensitization of cells to Dtxl [26]. As Fig. S10b (Supporting information) shown that the cell viability of PBA-Dtxl@MIL-101@BSA was 56.1% compared with 84.4% of PBA@MIL-101@BSA, 78.6% of Dtxl@MIL-101@BSA group and 88.2%

of MIL-101@BSA. The result confirmed that PBA enhanced the sensitization of tumor cells to Dtxl, realizing effectively killing tumor cells. Then, enhanced sensitization of cells to Dtxl due to PBA eliminating ER stress was further examined through the expression of apoptosis-associated proteins. The caspase 9 was chose in Western blot experiment. The caspase 9 was collected from 4T1 cells treated by 100 μg/mL of PBA@MIL-101@BSA, Dtxl@MIL-101@BSA, PBA-Dtxl@MIL-101@BSA for 24 h. According to the result shown in Fig. S10c (Supporting information), the activation of caspase 9 was significantly upregulated in PBA-Dtxl@MIL-101@BSA group compared with PBA@MIL-101@BSA and Dtxl@MIL-101@BSA groups. It demonstrated that PBA could enhance sensitization of tumor cells to Dtxl, causing overexpressing caspase 9 accelerated tumor cells apoptosis. The results proved that PBA-Dtxl@MIL-101 nanoparticles could assist ER alleviate ER stress, which enhanced the sensitization of cells to drugs for realizing effective tumor treatment.

HSP 90 as molecular chaperone could give assistance to refold misfolded or unfolded proteins from cell ER stress, which caused tumor recurrence [27,28]. PBA could inhibit the expression of the heat shock cognate protein [29]. Thence, it was significant strategy that PBA downregulating HSP 90 reduced ER stress for enhancing the efficiency of tumor treatment. To prove it, 4T1 cells were treated with PBA@MIL-101@BSA and MIL-101@BSA for 24 h and stimulated with 0.6 W MW for twice. As Fig. S10e (Supporting information) shown, the cell viability of MIL-101@BSA+MW group was higher than PBA@MIL-101@BSA+MW group, proving PBA could downregulate HSP 90. To further verify the effect of PBA on HSP 90, western blot experiment was employed. Fig. S10d (Supporting information) showed the activation of HSP 90 was obviously downregulated in PBA @MIL-101@BSA group compared with MIL-101@BSA group. It confirmed that PBA could downregulate HSP 90, which is helpful to hinder tumor recurrence under thermal stimulus.

Drug release experiment *in vitro* has verified that MW as exogenous stimulus could promote Dtxl to release efficiently. However, MIL-101 under MW stimulus could produce fever-type cell damage that made HSP overexpress, which led to tumor recurrence [30]. Hence PBA loaded into PBA-Dtxl@MIL-101 were used for eliminating ER stress response for reducing the process of HSP in tumor therapy. Additionally, MW as exogenous stimulus not only promoted the release of Dtxl and PBA but also controlled the release of Dtxl and PBA, which was further verified at the cellular level. As Fig. S10f (Supporting information) shown, the cells viability of MIL-101@BSA+MW group decreased from more 84% to 78% under MW heat stimulation, which confirmed that fever-type heat effect could slightly cause tumor cells death. Meanwhile, the cell survival rate of PBA-Dtxl@MIL-101@BSA group was less than Dtxl@MIL-101@BSA group due to PBA improving sensitization of tumor cells for Dtxl. What is more, the cell survival rate of PBA-Dtxl@MIL-101@BSA+MW group treated with twice MW at power of 0.6 W for 5 min was 37.4%. It indicated that MW promoted and controlled the release of drugs, realizing highly efficient tumor treatment accompanying with the effect of Dtxl and PBA. Figs. S11 and S12 (Supporting information) exhibited living and dead cell staining by Calcein-AM and propidium iodide (PI) and fluorescence staining images of cell morphology *via* Actin-Trakcer Green and 4′,6-diamidino-2-phenylindole. The results indicated that PBA-Dtxl@MIL-101@BSA under MW stimulus could destroy tumor cells effectively.

It was demonstrated that tumor cells were effectively destroyed owing to PBA improving sensitization of tumor cells for Dtxl and reducing the tolerance of tumor cells to heat by eliminating ER stress response. Therefore, the anti-tumor effect of PBA-Dtxl@MIL-101@BSA need be further verified *in vivo*. In our work, thirty female BALB/c mice with average weight of 18-25 g were divided into six groups, which was approved by the regulations of institutional animal care and use committee. 50 mg/kg of MIL-101@BSA, PBA@MIL-101@BSA, Dtxl@MIL1-101@BSA, PBA-Dtxl@MIL-101@BSA nanoparticles were injected in corresponding mice through the tail vein. Based on nanomaterials accumulating at the tumor site by enhanced permeability and retention effect, all tumor sites in MIL-101@BSA+MW and PBA-Dtxl@MIL-101@BSA+MW groups were stimulated by MW for 5 min (0.6 W) after 6 h postinjection. After another 2 h, these mice were treated by MW stimulus with the same condition. The MIL-101@BSA+MW group and the PBA-Dtxl@MIL-101@BSA+MW groups were recorded by the forward-looking infrared imaging instrument during MW stimulus (Fig. 3a). Fig. S13a (Supporting information) showed that the average temperature change was not obviously different in MIL-101@BSA+MW and PBA-Dtxl@MIL-101@BSA+MW groups. It confirmed that the temperature change between the two groups was not obvious, indicating that PBA and Dtxl played an important role on tumor treatment. The body weight change of tumor-bearing 4T1 mice after treatment, mice weight in different groups did not exhibit obviously different (Fig. S13b in Supporting information). Fig. 3b showed the change trend of tumor volume. The tumors in PBA-Dtxl@MIL-101@BSA+MW group was effectively inhibited compared with PBA-Dtxl@MIL-101@BSA and MIL-101@BSA+MW group, indicating that MW stimulus promoted really the release of PBA and Dtxl, PBA enhanced sensitization of tumor cells for Dtxl and reduce the tolerance of tumor cells to heat for inhibiting tumor recurrence. Additionally, the mean tumor volume of PBA-Dtxl@MIL-101@BSA group was the smaller than Dtxl@MIL-101@BSA group, further indicating that PBA enhanced sensitization of tumor cells for Dtxl. Fig. 3c showed that the survival rate of every group, the survival rate of PBA-Dtxl@MIL-101@BSA+MW group was up to 100%. Fig. S14a (Supporting information) showed that the pretreatment mice and mice treated for 15 days, which indicated that PBA-Dtxl@MIL-101@BSA under MW stimulus played excellent anti-tumor effect. After treating for 15 days, the main tissues of mice were collected and stained with H&E staining (spleen, liver, kidney, lung, and tumor) (Fig. S15 in Supporting information). As Fig S14b (Supporting information) shown that the degree of tumor necrosis of PBA-Dtxl@MIL-101@BSA+MW was the most serious, indicating that PBA-Dtxl@MIL-101@BSA under MW stimulus exhibited excellent anti-tumor effect.

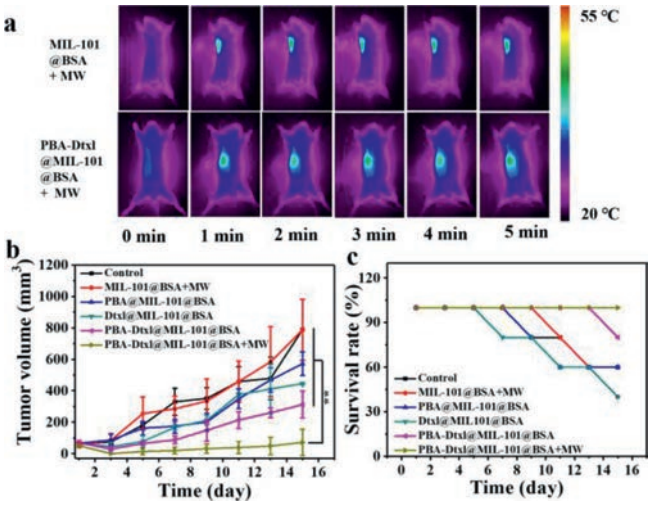

Fig. 3. Animal therapy experiment *in vivo*. (a) Infrared thermal images of mice treated with MIL-101 and PBA-Dtxl@MIL-101 under MW stimulus. (b) Tumor volume change curve of mice bearing 4T1 tumor treated with different treatment methods for 15 days. (c) Survival rate of mice treated with different treatment methods for 15 days. Scale bar is 50 μm. $^{**}P < 0.01$.

In conclusion, we designed and synthesized PBA-Dtxl@MIL-101@BSA nanoparticles as inhibitor of endoplasmic reticulum for sensitization of thermo-chemo therapy. The PBA-Dtxl@MIL-101 nanoparticles exhibited remarkable inhibitor effect of ER stress through upregulating caspase 9 proteins and reduce thermal tolerance by downregulating HSP 90. Moreover, we took advantage of MIL-101 nanoparticles as a pH and MW dual stimulus nanoplatform, which achieved the targeted release of PBA and Dtxl at tumor site. The results demonstrated that inhibition rate of tumor was up to more than 90%, exhibiting significant anti-tumor effect. It was demonstrated that the therapy sensitized by PBA-Dtxl@MIL-101 obviously destroyed tumor cells, showing simultaneously enhanced thermo-chemo therapy. Our work provided a promising strategy for tumor therapy by maximizing treatment efficacy and reducing treatment resistance.

Declaration of competing interest

The authors declare that they have no known competing financial interests or personal relationships that could have appeared to influence the work reported in this paper.

Acknowledgments

The authors acknowledge financial support from the Beijing Natural Science Foundation (No. 2202057), Sichuan Science and Technology Program (No. 2020YFSY0018).

Supplementary materials

Supplementary material associated with this article can be found, in the online version, at doi:10.1016/j.cclet.2021.09.084.

References

[1] W. He, S. Wang, J. Yan, et al., Adv. Funct. Mater. 29 (2019) 1807736.
[2] J. Xie, T. Fan, J.H. Kim, et al., Adv. Funct. Mater. 30 (2020) 20032391.
[3] X. Chen, J.R. Cubillos-Ruiz, Nat. Rev. Cancer 21 (2020) 1–18.
[4] Z. Tu, I.S. Donskyi, H. Qiao, et al., Adv. Funct. Mater. 30 (2020) 2000933.
[5] Y. Wang, S. Luo, C. Zhang, et al., Adv. Mater. 30 (2018) 1800475.
[6] B. Kaur, A. Bhat, R. Chakraborty, et al., Mol. Omics 14 (2018) 53–63.
[7] T. Yoshii, K. Mizusawa, Y. Takaoka, I. Hamachi, J. Am. Chem. Soc. 136 (2014) 16635–16642.
[8] K. Zhang, X. Meng, Y. Cao, et al., Adv. Funct. Mater. 28 (2018) 1804634.
[9] Y. Xing, T. Ding, Z. Wang, et al., ACS Appl. Mater. Interfaces 11 (2019) 13945–13953.
[10] Y. Wang, Q. Li, M. Deng, K. Chen, J. Wang, Chin. Chem. Lett. 33 (2022) 324–327 DOI:.
[11] H. Min, J. Wang, Y. Qi, et al., Adv. Mater. 31 (2019) 1808200.
[12] D. Zhang, M. Wu, Z. Cai, et al., Adv. Sci. 5 (2018) 1700648.
[13] Y. Yang, X. Ren, Z. Sun, et al., Chin. Chem. Lett. 29 (2018) 895–898.
[14] X. Pan, L. Bai, H. Wang, et al., Adv. Mater. 30 (2018) 1800180.
[15] J. Su, H. Sun, Q. Meng, et al., Theranostics 7 (2017) 523–537.
[16] W. Fan, B. Yung, P. Huang, X. Chen, Chem. Rev. 117 (2017) 13566–13638.
[17] M.R. Younis, C. Wang, R. An, et al., ACS Nano 13 (2019) 2544–2557.
[18] C. Fu, H. Zhou, L. Tan, et al., ACS Nano 12 (2018) 2201–2210.
[19] K.M.L. Taylor-Pashow, D.R. Joseph, X. Zhigang, T. Sylvie, L. Wenbin, J. Am. Chem. Soc. 131 (2009) 14261–14263.
[20] S.Y. Lee, E.H. Hong, J.Y. Jeong, et al., Biomater. Sci. 7 (2019) 4624–4635.
[21] B. Li, G. Hao, B. Sun, Z. Gu, Z.P. Xu, Adv. Funct. Mater. 30 (2020) 1909745.
[22] J. Liu, L. Tian, R. Zhang, et al., ACS Appl. Mater. Interfaces 10 (2018) 43493–43502.
[23] B. Kaur, A. Bhat, R. Chakraborty, et al., Mol. Omics. 14 (2018) 53–63.
[24] S. Ranga Rao, R. Subbarayan, S. Ajitkumar, D. Murugan Girija, J. Cell Physiol. 233 (2018) 60–66.
[25] Y.D. You, W.H. Deng, W.Y. Guo, et al., Dig. Dis. Sci. 64 (2019) 1535–1547.
[26] S. Shi, P. Tan, B. Yan, et al., Oncol. Rep. 35 (2016) 2606–2614.
[27] O. Grauer, M. Jaber, K. Hess, et al., J. Neurooncol. 141 (2019) 83–94.
[28] H. Luo, Q. Wang, Y. Deng, et al., Adv. Funct. Mater. 27 (2017) 1702834.
[29] R.C. Rubenstein, B.M. Lyons, Am. J. Physiol. Lung Cell Mol. Physiol. 281 (2001) L43–L51.
[30] H. Min, J. Wang, Y. Qi, et al., Adv. Mater. 31 (2019) 1808200.